Figure S1. Modeling of the MVA patient mutation *BUBR1*[L1012P] in mice

A) Gene targeting approach used to mimic the *BUBR1*[L1012P] MVA patient mutation at the corresponding residue in mice, *BubR1*[L1002P]. Shown are the relevant portions of the murine *BubR1* locus (top), the targeting construct (location of the L1002P mutation highlighted in red, top middle), recombined *BubR1*[L1002P] allele (bottom middle), and the final *BubR1*[L1002P] allele following Cre-recombinase mediated excision of the neomycin (Neo) cassette (bottom). The targeting vector was generated as follows. A genomic *BubR1* gene fragment of ~9.8 kb containing exons 20-23 was retrieved from BAC# bMQ_294E2 (129S7/SvEv ES Cell, Source BioScience) and transferred into pDTA (pDTA-BubR1 ex20-ex23). In order to introduce the CTT>CCT mutation, exon 23 was shuttled into pGEM-T using flanking BamHI sites, and mutagenesis was performed with Gene Tailor. The L>P modified exon 23 was then inserted into PL452 downstream of a loxP-neomycin phosphotransferase II (neo) gene-loxP cassette. Through PCR and recombineering, the loxP-neo-loxP L>P ex23 (~2.2 kb) was then cloned into pDTA-BubR1 ex20-ex23. The final targeting construct was linearized and electroporated into TL1 129Sv/E ES cells. Clones were selected and screened by Southern blotting analyses. **B)** Southern blot containing KpnI digested genomic DNA from two ES cell clones, hybridized with a PCR-generated 272 nt probe located in exon 20 (forward primer: 5'-ATCTGTAGAGAAAGACAAATTCAA G-3', reverse primer: 5'-CTATTATTTCATGAGTAACAAATTC-3'), showing the 6.6 and 8.5 kb fragments corresponding to the unmodified wildtype *BubR1* locus and the modified *BubR1*[L1002P] locus, respectively. **C)** PCR genotyping of *BubR1*^{+/+} and *BubR1*[+/L1002P] mice with the ~206 and ~293 bp amplicons corresponding with the wildtype and *BubR1*[L1002P] alleles, respectively. PCR primers were: forward: 5'-TAAGAGCAAGGCA CCTTAACCAA G-3', reverse: 5'-GAAATCCACTCTCGCCTGA GCC-3'.
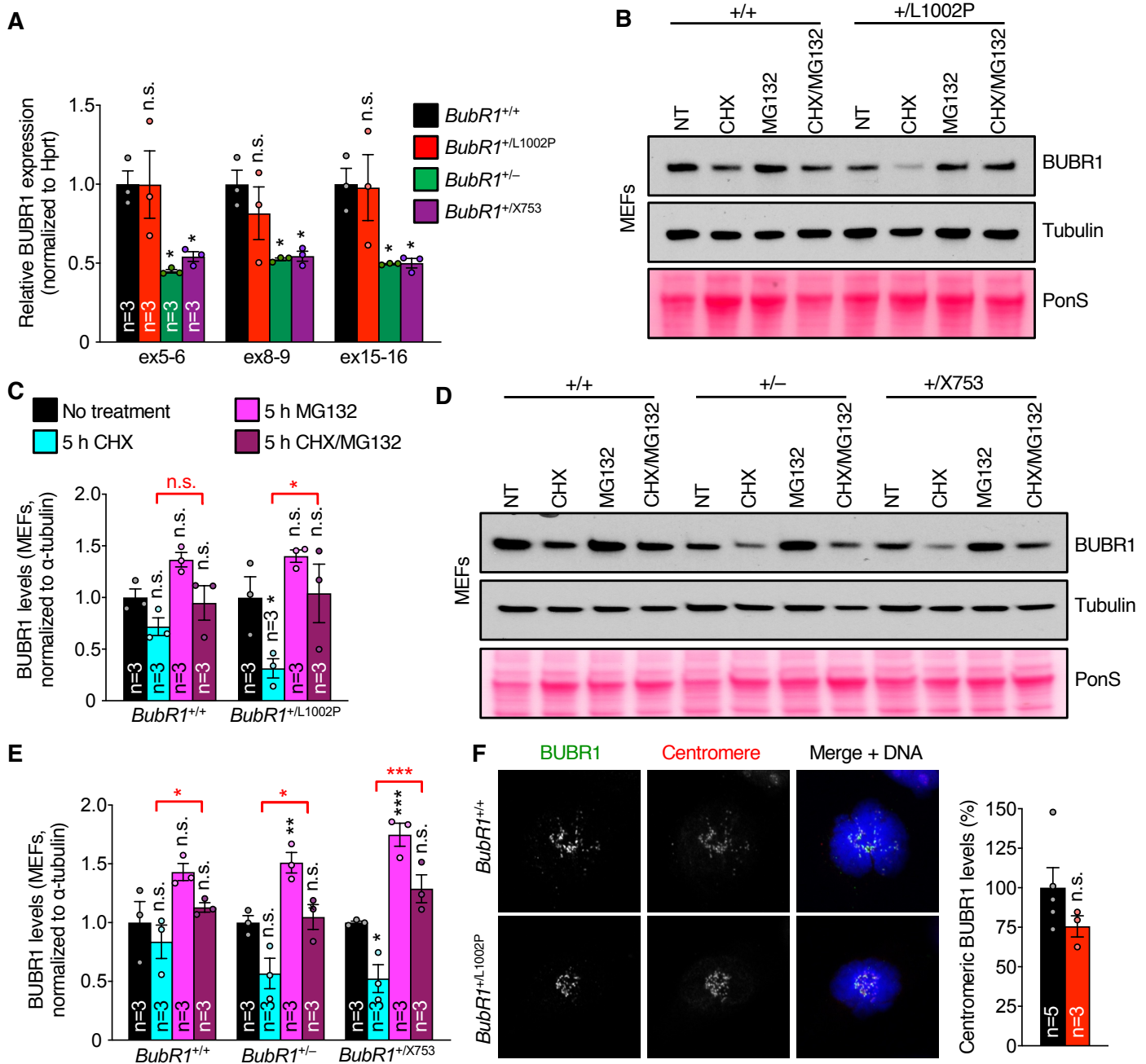
Figure S2. *BubR1*^L1002P and *BubR1*^X753 mutations differentially impact BUBR1 stability

A) Quantitative RT-PCR in indicated P5 MEFs. *BubR1* transcript levels were normalized to those of *Hprt*. Primer sequences used: *BubR1* ex5-6, forward 5'-GGATTGAACGCAAGGCTG-3', reverse 5'-CCATCTTCTTCCCTCT GCTC-3'; *BubR1* ex8-9 forward 5'-AATCCAGCCTCTGTGACG-3', reverse 5'-GTCTCCTTCTTCTCTCCCTG-3'; *BubR1* ex15-16 forward 5'-ATCACACTGTTCATCACCAG-3', reverse 5'-TGCCCCGTCATTAGTCAG-3'; *Hprt* forward 5'-TCATGGACTGATTATGGACAGG-3', reverse 5'-AATCCAGCAGGTCAGCAAAG-3'. **B)** Western blot of indicated P5 MEFs subject to no treatment (NT), treatment with the translation inhibitor cycloheximide (CHX), the proteasome inhibitor MG132, or both CHX and MG132 for 5 h. Blots were probed for BUBR1 and α-tubulin. Ponceau S and α-tubulin served as the loading controls. Three independent experiments were performed using three independent MEF lines per genotype. **C)** BUBR1 levels were quantified from experiments performed in **B** and were normalized to α-tubulin levels, with NT control for each genotype normalized to 1. **D)** Western blot of indicated P5 MEFs as in **B**. Blots were probed for BUBR1 and α-tubulin. Ponceau S and α-tubulin served as the loading controls. Three independent experiments were performed using three independent MEF lines per genotype. **E)** BUBR1 levels were quantified from experiments performed in **D** and were normalized to α-tubulin levels, as in **C**. **F)** Representative images of prometaphase MEFs labeled for BUBR1 and centromeres (left). Quantification of BUBR1 levels at the kinetochore in indicated MEFs, normalized to centromeric signal. N indicate independent MEF lines. Bars represent mean ± SEM (**A**, **C**, and **E-F**), and dots represent individual samples. Statistical significance was determined using a one-way ANOVA with a Holm-Sidak post-hoc test comparing all samples to each respective *BubR1*^+/+ (**A**) or NT control and CHX versus CHX/MG132 (**C** and **E**), and a 2-tailed unpaired *t* test (**F**) *$P<0.05$, **$P<0.01$, ***$P<0.001$. n.s., non-significant.
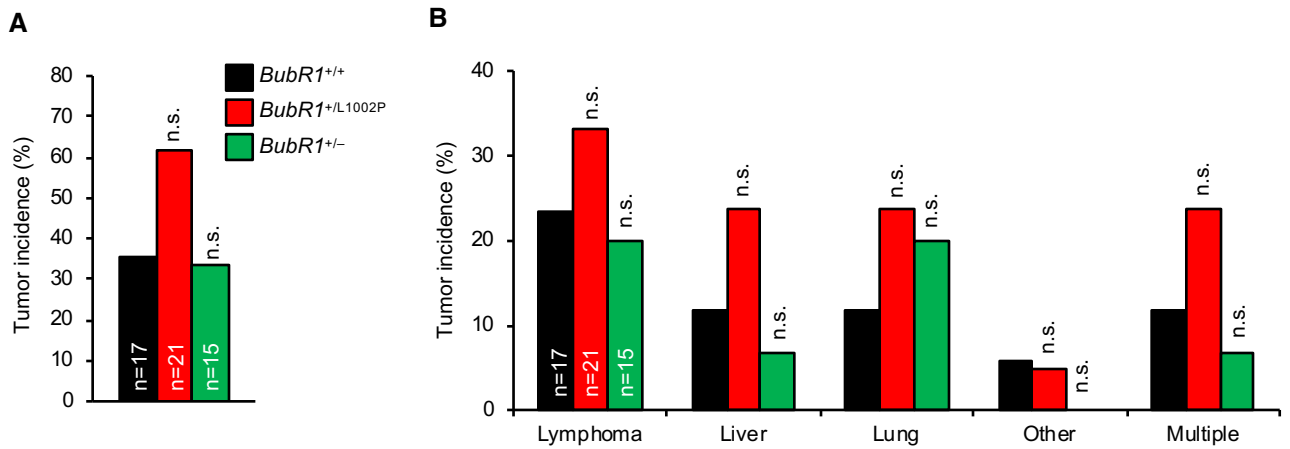
A)

B)

Figure S3. Spontaneous tumorigenesis in *BubR1*$^{+/L1002P}$ and *BubR1*$^{+/-}$ mice

A) Spontaneous tumor incidence in 18-20-month-old *BubR1*$^{+/+}$, *BubR1*$^{+/L1002P}$, and *BubR1*$^{+/-}$ mice. **B)** Spectrum of spontaneous tumor types observed. N indicate independent mice. Statistical significance was determined using a 2-tailed Fisher's exact text (**A-B**). n.s., non-significant.
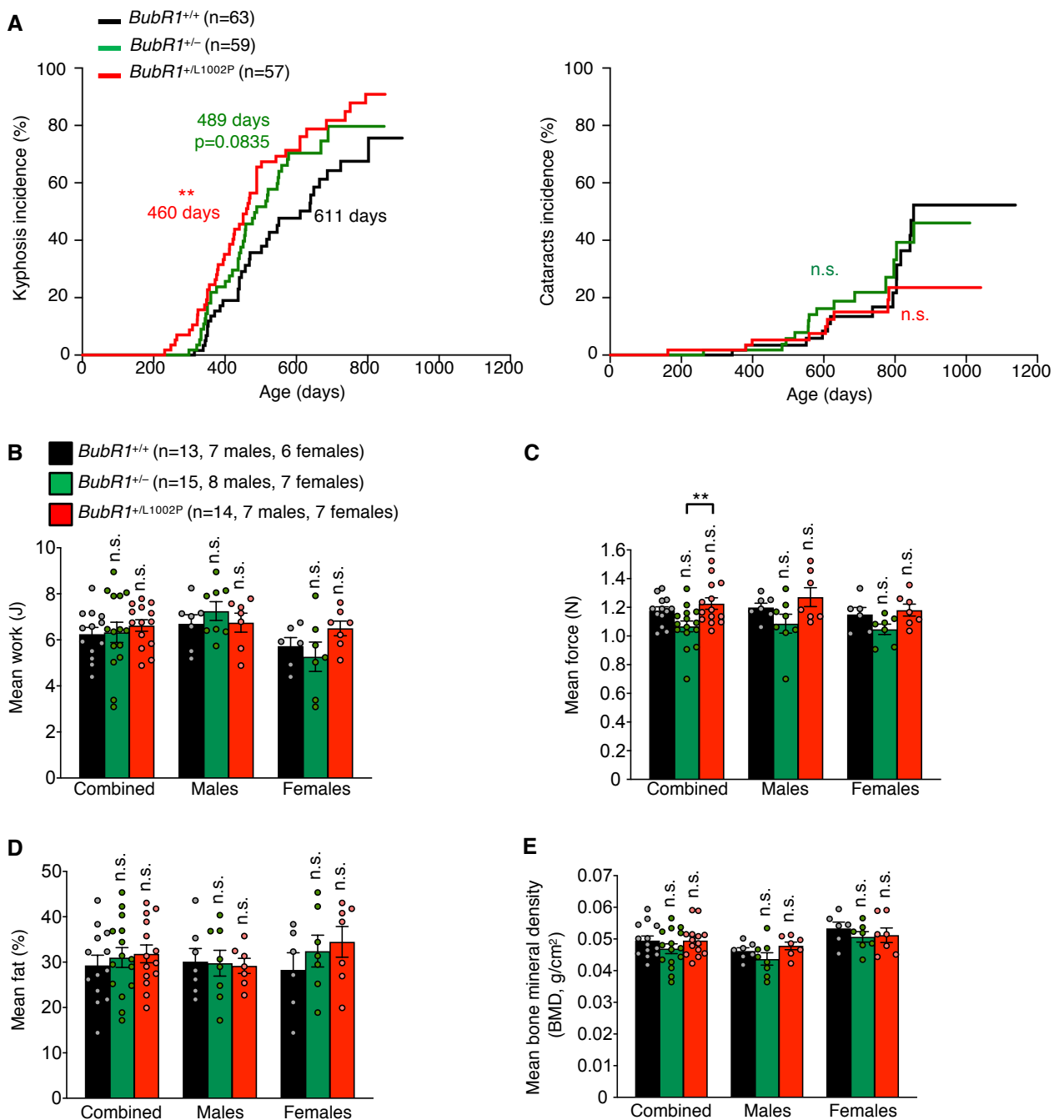
Figure S4. *BubR1^{+/L1002P}* and *BubR1^{+/–}* mice show little evidence of progeria

A) Kaplan-Meier curves of kyphosis (left) and cataracts (right) onset in *BubR1^{+/+}*, *BubR1^{+/L1002P}*, and *BubR1^{+/–}* mice. Values associated with curves denote median onset of kyphosis or cataracts. **B)** Mean work output, in joules (J), during a treadmill exercise test of 16-18-month-old mice. **C)** Analysis of mean forelimb grip strength in 16-18-month-old *BubR1^{+/+}*, *BubR1^{+/L1002P}*, and *BubR1^{+/–}* mice. Animal numbers are indicated in B. **D)** Mean total body fat percentage of 16-18-month-old mice, as determined by echo-MRI analyses. Animal numbers are indicated in B. **E)** Mean total body bone mineral density (BMD) of 16-18-month-old mice, as determined by DEXA scanning. Animal numbers are indicated in B. N indicate independent mice for all experiments. Bars in **B-E** represent mean ± SEM, and dots represent individual samples. Statistical significance was determined using a one-way ANOVA with a Holm-Sidak post-hoc test (**B-E**). **P<0.01. n.s., non- significant.
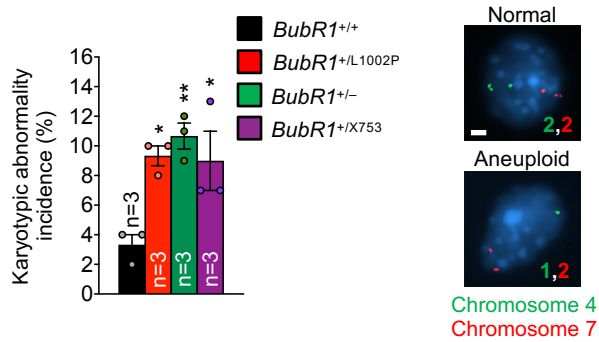
Figure S5. MVA allele carriers exhibit similar aneuploidy rates

Percentage of cells exhibiting karyotypic abnormalities, as determined by observation of nonmodal chromosome 4 (green) and/or 7 (red) signals using FISH analyses. P6 MEFs were used for analyses. Representative images shown to right. Scale bar, 2 μm. N indicate independent MEF lines. Bars represent mean $\pm$ SEM, and dots represent individual samples. Statistical significance was determined using a one-way ANOVA with a Holm-Sidak post-hoc test. *$P<0.05$ and **$P<0.01$.
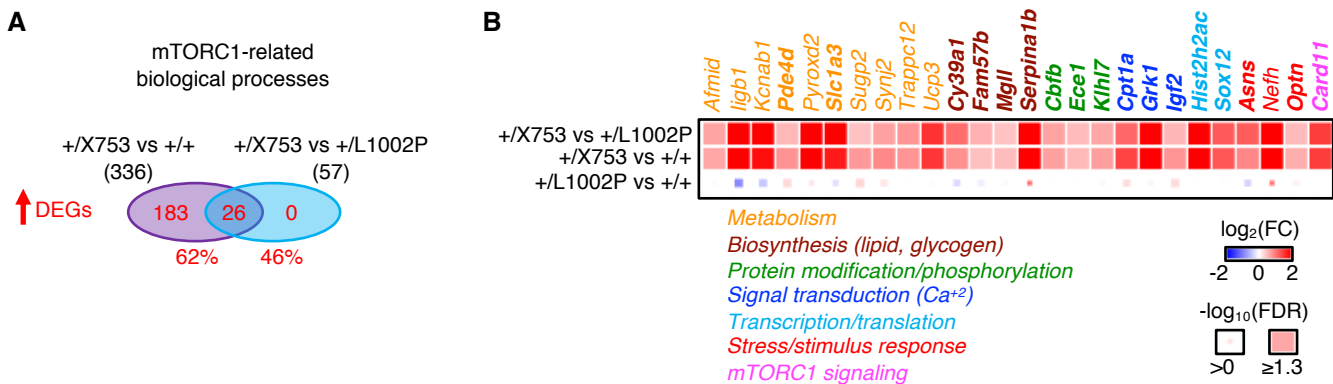
A mTORC1-related biological processes

B

Figure S6. Progeroid *BubR1*[+/X753] mice exhibit hyperactive mTORC1 signaling

A) Venn diagrams of significantly DEGs present in mTORC1-related gene sets from the functional enrichment analyses in Figure 4B, from the RNA sequencing analyses of 3-month-old skeletal muscle (gastrocnemius) from the indicated mice. ↑, upregulated genes. Gene numbers in parentheses represent total DEGs. Percentages below represent mTORC1-related genes in dataset. **B)** Heatmap of expression of the 26 mTORC1-related genes upregulated in the *BubR1*[+/X753] vs. *BubR1*[+/L1002P] comparison shown in **A**. Gene names in bold text denote genes associated with multiple mTORC1-related biological processes. N=3 independent mice/genotype were used for analyses.
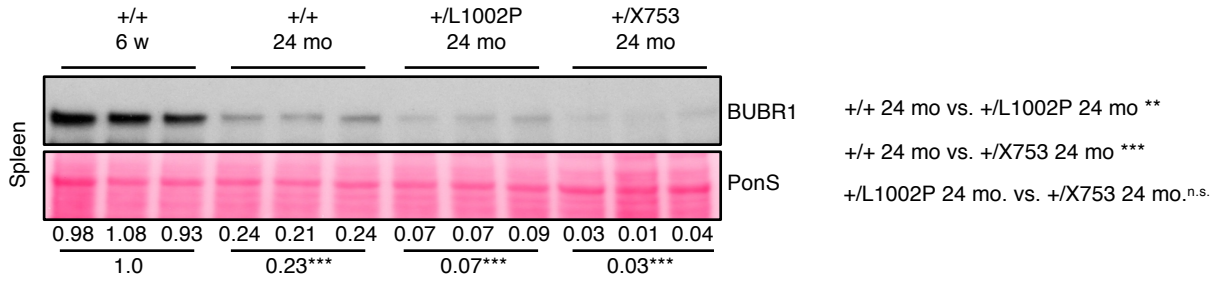
	+/+ 6 w			+/+ 24 mo			+/L1002P 24 mo			+/X753 24 mo		
BUBR1												
PonS												
	0.98	1.08	0.93	0.24	0.21	0.24	0.07	0.07	0.09	0.03	0.01	0.04
		1.0			0.23***			0.07***			0.03***	

+/+ 24 mo vs. +/L1002P 24 mo **

+/+ 24 mo vs. +/X753 24 mo ***

+/L1002P 24 mo. vs. +/X753 24 mo.n.s.

Figure S7. MVA allele carriers exhibit a similar age-related decline in BUBR1

Western blots of spleen lysates from 6-week-old *BubR1*^{+/+} (left) and 24-month-old *BubR1*^{+/+}, *BubR1*[+/L1002P], and *BubR1*[+/X753] (right) mice probed for BUBR1. Total protein, determined by PonS, served as the loading control. Three independent mice were used for analyses. BUBR1 levels were quantified and normalized to PonS levels. Values below the images represent the quantified BUBR1 levels, with the 6-week-old *BubR1*^{+/+} samples normalized to 1. Values below the line represent the mean. N indicate independent mice. Statistical significance was determined using a one-way ANOVA with a Holm-Sidak post-hoc test. **$P<0.01$, ***$P<0.001$. n.s., non- significant.
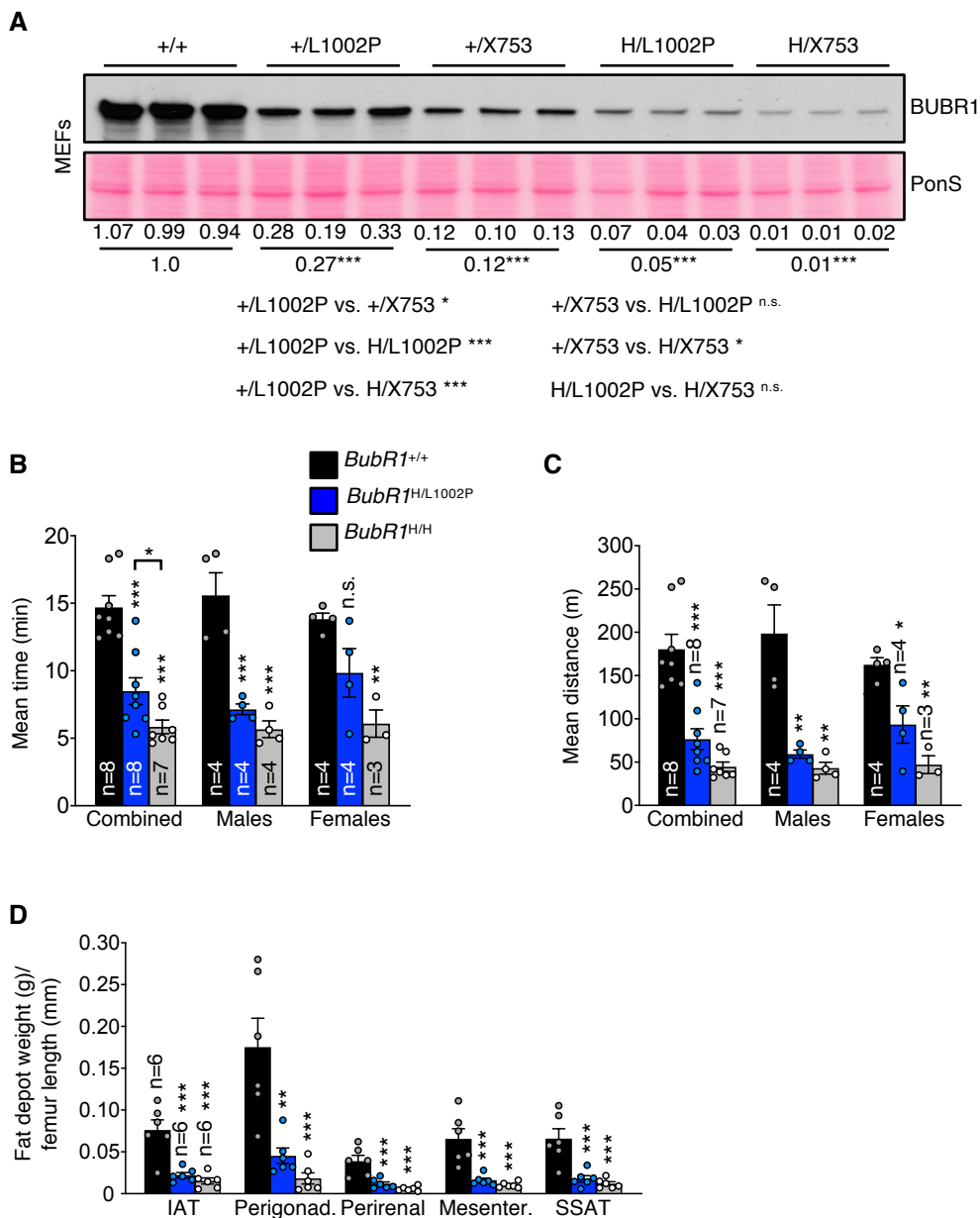
Figure S8. Analysis of progeroid phenotypes of viable MVA models

A) Western blot of P5 *BubR1*^{+/+}, *BubR1*[+/L1002P], *BubR1*[+/X753], *BubR1*[H/L1002P], and *BubR1*[H/X753] MEF lysates probed for BUBR1. Total protein, determined by PonS, served as the loading control. Three independent lines were used for analyses. BUBR1 levels were quantified and normalized to PonS levels. Values below the images represent the quantified BUBR1 levels, with *BubR1*^{+/+} normalized to 1. Values below the line represent the mean. **B)** Total running time (to exhaustion, min.) during a treadmill exercise test in 5-7-month-old mice. **C)** Total running distance (m) during a treadmill exercise test in 5-7-month-old mice. **D)** Individual gross fat depot weights (g) from 8-10-month-old *BubR1*^{+/+}, *BubR1*[H/L1002P], and *BubR1*[H/H] mice, normalized to right femur length (mm). N indicate independent mice for all experiments. Bars represent mean ± SEM (**B-C**), and dots represent individual samples. Statistical significance was determined using a one-way ANOVA with a Holm-Sidak post-hoc test. *$P<0.05$, **$P<0.01$, and ***$P<0.001$. n.s., non-significant.
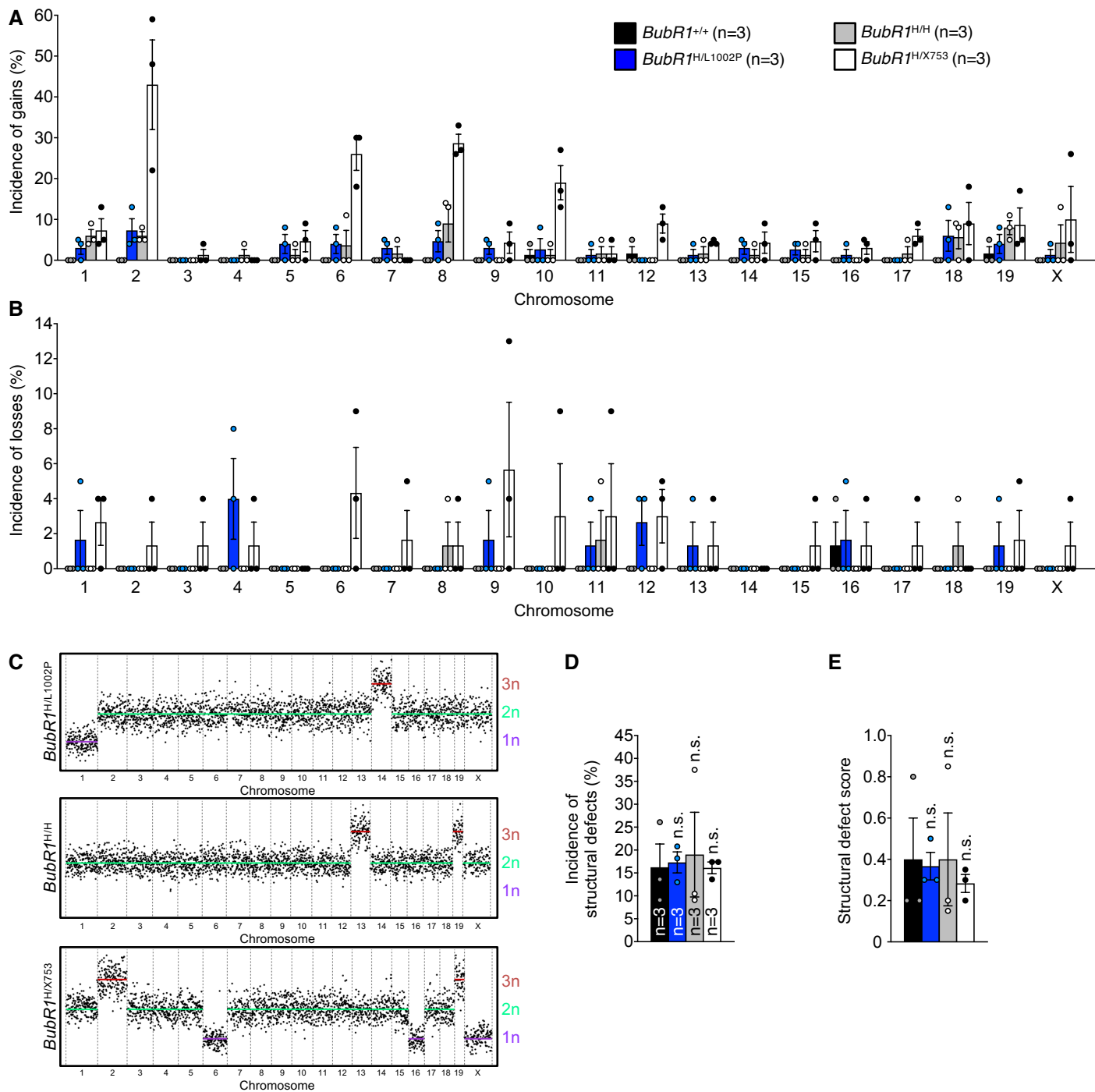
Figure S9. Aneuploidization impacts viability, but not progeria in biallelic MVA mutants.

A) Distribution of whole chromosomes gained in P5 *BubR1*^{+/+}, *BubR1*[H/L1002P], *BubR1*[H/H], and *BubR1*[H/X753] MEFs, as determined by single cell DNA sequencing. **B)** Distribution of chromosomes lost in biallelic MVA MEFs, as in **A**. **C)** Representative single cell DNA sequencing profiles for *BubR1*[H/H], *BubR1*[H/L1002P], and *BubR1*[X/753] MEFs. **D)** Incidence of structural defects or segmental aneuploidy in biallelic MVA MEFs, as determined by partial chromosome loss or gain by single cell DNA sequencing. **E)** Structural defect scores, representing the number of copy number transitions for partial chromosome modifications only, for biallelic MVA MEFs, as determined by single cell DNA sequencing. N indicate independent lines, and N represented in **A** apply to all panels. See methods for further details on data analysis. Bars in **A-B** and **D-E** represent mean ± SEM, and dots represent individual samples. A one-way ANOVA with a Holm-Sidak post-hoc test was used to assess significance (**D-E**). n.s., non-significant.
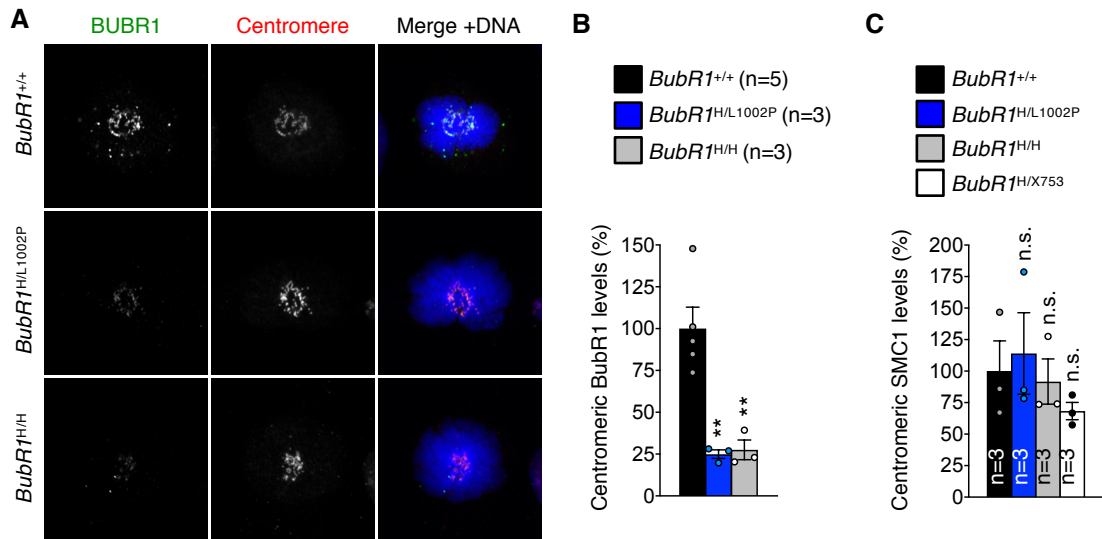
Figure S10. Heterogeneity among MVA models occurs despite mitotic similarity

A) Representative images of prometaphase MEFs labeled for BubR1 and centromeres. **B)** Quantification of BubR1 levels at the kinetochore in *BubR1*^{+/+}, *BubR1*[H/L1002P] and *BubR1*[H/H] MEFs, normalized to centromeric signal. N indicate independent lines. *BubR1*^{+/+} controls are as shown in Figure S2F. **C)** Quantification of SMC1 levels at the kinetochore in *BubR1*^{+/+}, *BubR1*[H/L1002P], *BubR1*[H/H], and *BubR1*[H/X753] MEFs, normalized to centromeric signal. N indicate independent lines. Bars represent mean $\pm$ SEM, and dots represent individual samples. Statistical significance was determined using a one-way ANOVA with a Holm-Sidak post-hoc test. **$P<0.01$. n.s., non-significant.

	+/+	+/X573	+/L1002P	X753/L1002P	Total
Newborn	137	128	123	0	388
E13.5	19	9	11	0	39
E3.5	8	3	6	3	20

Table S1. Mice modeling MVA patient *BUBR1*[X753/L1012P] are embryonic lethal

Yield of the indicated mice at various ages. Newborn, postnatal day 0. Embryonic day (E).

Mitotic MEF genotype (n)	Mitotic figures inspected	Percent aneuploid figures (s.d.)	Karyotypes with indicated chromosome number										Percent mitotic figures with PCS (s.d.)
			36	37	38	39	40	41	42	43	44	45	
BubR1^{+/+} (3)	150	8 (0)			4	2	138	6					0 (0)
BubR1^{+/L1002P} (3)	150	23 (2)***			7	11	116	12	4				9 (1)***
BubR1^{+/−} (3)	150	19 (1)***			9	5	121	12	3				8 (3)***
BubR1^{+/GTTA} (3)	250	19 (1)***			6	8	121	11	3	1			10 (2)***
BubR1^{+/+} (3)	150	12 (2)		1	2	5	132	7	3				3 (1)
BubR1^{H/L1002P} (3)	150	39 (3)***	1	1	6	17	91	18	14		1	1	75 (2)***
BubR1^{H/H} (3)	125	36 (6)***			5	13	80	20	6	1			15 (3)***
BubR1^{H/GTTA} (3)	150	65 (3)***		7	8	11	52	26	23	16	7		76 (3)***

Table S2. *BubR1* MVA allele carriers and biallelic mutant MEFs exhibit aneuploidy

Karyotype analysis of numerical chromosomal abnormalities in mitotic P5 MEFs from *BubR1* MVA allele carriers and biallelic mutants. Data represent the mean ± standard deviation (s.d.) Statistical significance was determined using a one-way ANOVA with a Holm-Sidak post-hoc test. ***$P<0.001$.

Tissue type	Genotype (n)	Percentage of Aneuploidy (SEM)			Percentage tetraploidy (SEM)	Percentage polyploidy (SEM)
		Chr. 4	Chr. 7	Chr. 4/7	Chr. 4/7	Chr. 4/7
MEFs (P5)	*BubR1*^{+/+} (3)	2.3 (0.7)	3.0 (1.2)	3.3 (0.7)	11.0 (3.2)	0 (0)
	BubR1[+/L1002P] (3)	7.0 (0.6)[n.s.]	4.7 (1.2)[n.s.]	9.3 (0.7)*	10.7 (1.9)[n.s.]	0 (0)
	BubR1^{+/−} (3)	7.0 (1.0)[n.s.]	5.3 (0.9)[n.s.]	10.7 (0.9)**	7.7 (2.0)[n.s.]	0 (0)
	BubR1[+/X753] (3)	6.7 (1.8)[n.s.]	5.3 (1.3)[n.s.]	9.0 (2.0)*	9.3 (3.0)[n.s.]	0 (0)
Liver (24 mo.)	*BubR1*^{+/+} (3)	13.3 (4.1)	7.7 (2.2)	16 (5.3)	27.0 (13.3)	3.3 (1.7)
	BubR1[+/L1002P] (3)	30.7 (1.9)*	22.7 (5.2)[n.s.]	46.7 (4.3)**	30.3 (4.6)[n.s.]	1.7 (0.3)[n.s.]
	BubR1^{+/−} (3)	28.7 (3.2)*	23.0 (1.2)[n.s.]	41.7 (3.2)**	31.0 (4.2)[n.s.]	2.3 (1.9)[n.s.]
	BubR1[+/X753] (4)	16.3 (1.7)[n.s.]	15.0 (3.3)[n.s.]	24.5 (3.0)[n.s.]	27.8 (2.5)[n.s.]	4.8 (1.5)[n.s.]
Lung (24 mo.)	*BubR1*^{+/+} (5)	2.2 (0.5)	1.8 (0.6)	4.8 (1.0)	3.8 (1.9)	0 (0)
	BubR1[+/L1002P] (3)	7.7 (0.3)**	5.0 (1.7)[n.s.]	11.3 (1.2)*	1.0 (0)[n.s.]	0 (0)
	BubR1^{+/−} (3)	4.7 (0.9)[n.s.]	5.0 (1.2)[n.s.]	9.0 (2.0)[n.s.]	1.7 (0.7)[n.s.]	0 (0)
	BubR1[+/X753] (4)	7.3 (1.0)**	7.0 (1.3)*	12.5 (1.3)**	1.8 (0.5)[n.s.]	0 (0)
Spleen (24 mo.)	*BubR1*^{+/+} (3)	2.3 (0.6)	2.3 (1.5)	4.7 (0.7)	0 (0)	0 (0)
	BubR1[+/L1002P] (3)	5.0 (2.0)[n.s.]	5.0 (2.3)[n.s.]	9.7 (2.7)[n.s.]	0 (0)[n.s.]	0 (0)
	BubR1^{+/−} (3)	4.0 (1.7)[n.s.]	6.0 (0.6)[n.s.]	9.7 (2.0)[n.s.]	0.3 (0.3)[n.s.]	0 (0)
	BubR1[+/X753] (4)	5.5 (1.3)[n.s.]	5.5 (1.0)[n.s.]	9.8 (0.8)[n.s.]	2.5 (1.6)[n.s.]	0 (0)
Sk. Muscle (Gastro., 8-10 mo.)	*BubR1*^{+/+} (4)	2.0 (0.7)	2.0 (0.7)	4.0 (0.9)	0.3 (0.3)	0 (0)
	BubR1[H/L1002P] (4)	9.0 (0.8)***	5.8 (1.3)*	13.5 (0.3)***	0.8 (0.5)[n.s.]	0 (0)
	BubR1[H/H] (4)	9.5 (1.0)***	6.0 (0.7)*	11.8 (1.5)***	0.8 (0.3)[n.s.]	0 (0)
Fat (IAT, 8-10 mo.)	*BubR1*^{+/+} (4)	3.3 (0.8)	2.8 (0.5)	5.8 (0.6)	0.3 (0.3)	0 (0)
	BubR1[H/L1002P] (4)	8.8 (2.3)[n.s.]	7.8 (1.1)*	15.5 (2.4)**	0.5 (0.3)[n.s.]	0 (0)
	BubR1[H/H] (4)	4.5 (1.3)[n.s.]	6.0 (1.1)[n.s.]	10.3 (1.3)[n.s.]	0.5 (0.3)[n.s.]	0 (0)
Heart (8-10 mo.)	*BubR1*^{+/+} (4)	3.8 (0.6)	6.0 (0.7)	6.5 (0.6)	11.0 (2.2)	0.5 (0.3)
	BubR1[H/L1002P] (4)	15.3 (3.0)**	12.3 (1.3)**	18.5 (2.8)**	10.0 (1.4)[n.s.]	0.8 (0.8)[n.s.]
	BubR1[H/H] (4)	9.3 (1.4)[n.s.]	8.0 (0.9)[n.s.]	13.5 (1.3)*	6.5 (1.6)[n.s.]	0 (0)[n.s.]
Kidney (8-10 mo.)	*BubR1*^{+/+} (4)	4.0 (1.3)	2.5 (0.3)	6.0 (0.9)	0.3 (0.3)	0 (0)
	BubR1[H/L1002P] (4)	13.5 (1.2)***	12.0 (1.4)**	22.0 (1.6)***	3.5 (0.6)[n.s.]	0 (0)
	BubR1[H/H] (4)	11.0 (0.4)**	14.3 (1.8)***	20.5 (1.8)***	5.5 (1.6)*	0 (0)
Spleen (8-10 mo.)	*BubR1*^{+/+} (4)	2.8 (0.5)	1.3 (0.6)	3.8 (0.9)	0.5 (0.5)	0 (0)
	BubR1[H/L1002P] (4)	7.0 (2.3)[n.s.]	7.5 (0.9)***	13.8 (1.9)**	0.3 (0.3)[n.s.]	0 (0)
	BubR1[H/H] (4)	5.0 (0.7)[n.s.]	5.0 (0.4)**	9.5 (0.6)*	0 (0)[n.s.]	0 (0)

Table S3. *BubR1* MVA allele carriers and biallelic mice exhibit mosaic aneuploidy

Interphase FISH analyses, using probes for chromosomes 4 and 7, of P5 MEFs, and liver, lung, and spleen from 24-month-old *BubR1* MVA allele carriers (*BubR1*[+/L1002P], *BubR1*^{+/−}, and *BubR1*[+/X753]) and skeletal muscle (sk. muscle, gastrocnemius), fat (IAT), heart, kidney, and spleen from 8-10-month-old biallelic *BubR1* MVA mutant mice (*BubR1*[H/L1002P] and *BubR1*[H/H]). Tetraploidy, 4n for both chromosomes 4 and 7. Polyploidy, >4n for both chromosomes 4 and 7, 8n, 16n, etc. Data represent the mean ± SEM. Statistical significance was determined using a one-way ANOVA with a Holm-Sidak post-hoc test. *$P<0.05$, **$P<0.01$, ***$P<0.001$. n.s., non-significant.

Mitotic Splenocyte genotype (n)	Mitotic figures inspected	Percent aneuploid figures (s.d.)	Karyotypes with indicated chromosome number										Percent mitotic figures with PCS (s.d.)
			36	37	38	39	40	41	42	43	44	45	
BubR1$^{+/+}$ (3)	150	1 (1)				1	149						0 (0)
BubR1$^{+/L1002P}$(3)	150	28 (2)***	1	3	4	11	108	13	7	2	1		14 (2)***
BubR1$^{+/-}$ (3)	100	2 (2)$^{n.s.}$				1	98	1					0 (0)$^{n.s.}$
BubR1$^{+/GTTA}$ (3)	150	18 (2)***			3	11	123	9	2	2			14 (2)***
BubR1$^{H/L1002P}$ (3)	140	38 (6)***		7	12	9	87	18	7				55 (10)***
BubR1$^{H/H}$ (4)	200	15 (4)**			2	12	170	16					36 (6)*

Table S4. Mono- and biallelic *BubR1* MVA mice exhibit diversity in aneuploidy

Karyotype analysis of numerical chromosomal abnormalities in mitotic splenocytes from 5-month-old mono- and biallelic *BubR1* MVA mice. Data represent the mean ± s.d. Statistical significance was determined using a one-way ANOVA with a Holm-Sidak post-hoc test. *$P<0.05$, **$P<0.01$, ***$P<0.001$. n.s., non-significant.

| MVA Models | BUBR1 levels (%) | | % Aneuploidy | | | | | | | | | | Cancer Phenotypes | | Progeroid Phenotypes | | | |
| | | | Karyotyping (mitotic) | | FISH (interphase) | | | | | | | | | | | | | |
BubR1 genotype	In vitro	In vivo (spleen)	In vitro	In vivo (spleen)	Liver 24 m	Lung 24 m	Spleen 24/10 m	Kidney 10 m	Heart 10 m	Fat 10 m	Sk.M 10 m	Cancer Survival (d)	DMBA-induced	Survival (d)	Sarcopenia (kyphosis-median onset)	Lipodystrophy (age assessed)	Cataracts (median onset)
+/+	100	100	8\12	1	16	5	5\4	6	7	6	4	902	~50% incidence (lung)	886	No	No	No
Monoallelic																	
+/L1002P	39***	16***	23***	28***	47**	11*	10	N.E.	N.E.	N.E.	N.E.	809	↑ tumor vol.	770	No- mild (460 vs. 611 d)**	No	No
+/−	10***	9***	19***	2	42**	9	10	N.E.	N.E.	N.E.	N.E.	816	↑ tumor vol./num.	741	No- mild (489 vs. 611 d)	No	No
+/X753	25***	14***	19***	18***	25	13**	10	N.E.	N.E.	N.E.	N.E.	No	↑ tumor vol.	665	Yes (623 vs. 812 d)***	Yes (720 d)	Yes (707 vs. 812 d)*
Biallelic																	
H/L1002P	5***\18***	13***	39***	38***	N.E.	N.E.	14**	22***	19**	16**	14***	N/A	↑ inc./vol./num.	343	Yes (238 vs. 571 d)***	Yes (240-300 d)	Yes (161 vs. 974 d)***
H/H	25***	3***	36***	15**	N.E.	N.E.	10*	21***	14*	10	12***	N/A	↑ inc./num.	196	Yes (175 vs. 571 d)***	Yes (240-300 d)	Yes (168 vs. 974 d)***
H/X753	5**\1***	N.E.	65***	N/A	N.E.	N.E.	N.E.	N.E.	N.E.	N.E.	N.E.	N/A	N/A	1	N/A	N/A	N/A
–/H	13**	N.E.	72	N/A	N.E.	N.E.	N.E.	N.E.	N.E.	N.E.	N.E.	N/A	N/A	1	N/A	N/A	N/A
X753/L1002P	N/A	N/A	N/A	N/A	N/A	N/A	N/A	N/A	N/A	N/A	N/A	N/A	N/A	E3.5	N/A	N/A	N/A

Table S5. *BubR1* MVA mono- and biallelic mice exhibit phenotypic diversity independent of BUBR1 levels and aneuploidy rates

Summary of *BubR1* MVA mouse model phenotypes, including BUBR1 protein levels, aneuploidy rates, and cancer and progeroid phenotypes. Abbreviations: m, months; Sk.M, skeletal muscle; d, days; inc., incidence; vol., volume; num., number; N.E., not evaluated; N/A, not applicable.